Plasma Sci. Technol. **19** (2017) 064002 (10pp) https://doi.org/10.1088/2058-6272/aa6153

Impedance matching for repetitive high voltage all-solid-state Marx generator and excimer DBD UV sources

Yonggang WANG (王永刚), Liqing TONG (童立青)[1] and Kefu LIU (刘克富)

Institute of Electrical Light Source, Fudan University, Shanghai 200433, People's Republic of China

E-mail: tonglq@fudan.edu.cn

Received 28 December 2016, revised 13 February 2017
Accepted for publication 14 February 2017
Published 28 April 2017

Abstract

The purpose of impedance matching for a Marx generator and DBD lamp is to limit the output current of the Marx generator, provide a large discharge current at ignition, and obtain fast voltage rising/falling edges and large overshoot. In this paper, different impedance matching circuits (series inductor, parallel capacitor, and series inductor combined with parallel capacitor) are analyzed. It demonstrates that a series inductor could limit the Marx current. However, the discharge current is also limited. A parallel capacitor could provide a large discharge current, but the Marx current is also enlarged. A series inductor combined with a parallel capacitor takes full advantage of the inductor and capacitor, and avoids their shortcomings. Therefore, it is a good solution. Experimental results match the theoretical analysis well and show that both the series inductor and parallel capacitor improve the performance of the system. However, the series inductor combined with the parallel capacitor has the best performance. Compared with driving the DBD lamp with a Marx generator directly, an increase of 97.3% in radiant power and an increase of 59.3% in system efficiency are achieved using this matching circuit.

Keywords: impedance matching circuit, all-solid-state Marx generator, DBD lamp

(Some figures may appear in colour only in the online journal)

1. Introduction

Dielectric barrier discharges (DBDs) are widely used in various applications, such as surface treatment, ozone generation, depollution of gas streams, wastewater treatment, and excimer DBD ultraviolet (UV) sources [1–8]. $KrCl^*$ excimer sources can emit an intense narrow-band UV radiation at 222 nm using DBD. In addition, the 222 nm radiation has been proved to make a significant contribution to water purification, air deodorization, and so on [9].

DBDs are traditionally driven by sinusoidal voltages. In recent years, pulsed operation of DBDs was found to be superior in terms of discharge homogeneity and energy efficiency [10–17]. Liu and Neiger studied DBDs driven by unipolar square pulses [11]. It was found that compared with sine wave excitation, an improvement of about 30% in energy efficiency is achieved for ozone synthesis. Afterwards, intensive work has been done to compare the performance of DBDs driven by various voltage waveforms in wide fields including ozone generation, vacuum ultraviolet radiation, plasma jet plume, atmospheric air discharge, etc [12–17]. This research demonstrated that DBDs excited by square pulses have superior performance compared with those excited by sinusoidal voltages, especially in energy efficiency.

However, the energy efficiency is based on the energy input into DBD reactors, which is calculated by integrating the product of measured external voltage and current in the case of pulse excitation. The efficiency of pulsed power supplies (PSs) to DBD reactors is seldom considered. According to Han [7], the power delivered to the $KrBr^*$ excimer DBD lamp is merely 40% of the PS output power in the case of pulsed PS, and approximately 70% in the case of rectangular and sinusoidal PSs. In order to improve system efficiency, an impedance matching circuit should be inserted between the PS and DBD reactor.

[1] Author to whom any correspondence should be addressed.

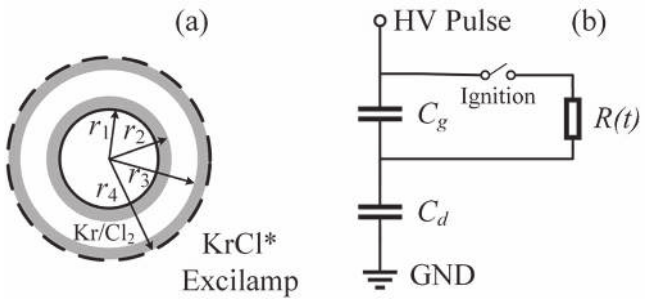

Figure 1. Schematic diagram of the KrCl* excimer DBD lamp: (a) cross sectional configurations, (b) equivalent electrical model.

Impedance matching is well studied for DBDs excited by sinusoidal PSs [18–20]. In general, a circuit composed of passive components (inductors, capacitors and/or resistors) is added between the sinusoidal PS and DBD reactor to make the impedance of the whole load resistive, seen by the output terminals of the PS. If a matching frequency is given and values of some components are chosen, the values of the rest elements can be calculated. However, there are no matching frequencies for DBDs driven by pulsed voltage. Hence, it is unable to be employed here. There are also numerous articles about the issue of matching a DBD reactor to a pulsed PS [21, 22]. But in these works, pulse voltages are delivered to the DBD reactors through transmission lines. Thus the impedance matching techniques and matching networks are not suitable for the matching of pulse voltage converter and DBD reactor. Therefore, new impedance matching techniques must be developed.

In our previous work, an inductor was inserted between pulse generator and KrCl* excimer DBD lamp [23]. It demonstrates that with the help of the inductor, the radiant power becomes larger and system efficiency higher though with the same input power. However, more detailed work has not been done.

In this paper, we first introduce load characteristics and the pulse generator briefly in section 2, and then analyze various impedance matching circuits in section 3. In order to verify the theoretical analysis, experiments with these matching circuits are conducted. The experimental set-up is described in section 4, and the experimental results are presented and discussed in section 5. Finally, the conclusion is made in section 6.

2. Load characteristics and pulse generator

2.1. Load characteristics

A schematic diagram of the KrCl* excimer DBD lamp is illustrated in figure 1(a). Coaxial geometry is adopted. r_1 and r_2 are the inner and outer radius of the inner quartz tube, while the inner and outer radius of the outer quartz tube are r_3 and r_4, respectively. The high voltage electrode is composed of two pieces of stainless steel foil, which are attached firmly to the inner surface of the inner tube. The outer surface of the outer tube is wrapped in a ring metal mesh that is grounded. Chlorine and krypton are filled in the annular discharge cavity. The effective discharge length L_D is 14 cm.

Table 1. KrCl* excilamp parameters and capacitance values.

Parameters	Value	Parameters	Value
r_1	13.5 mm	r_2	15 mm
r_3	18.5 mm	r_4	20 mm
L_D	14 mm	ε_r	3.7
C_g	37.1 pF	$C_{d,inner}$	273.52 pF
$C_{d,outer}$	369.64 pF	C_d	157.20 pF
C_{DBD}	30.04 pF		

The equivalent electrical model of the DBD lamp is shown in figure 1(b). C_g and C_d represent the equivalent capacitance of gap and dielectric layer respectively. The equivalent capacitance of the gas gap is

$$C_g = \frac{2\pi\varepsilon_0 L_D}{\ln(r_3/r_2)}. \tag{1}$$

C_d is the total series capacitance of the inner and outer dielectric layers, i.e.

$$\begin{aligned} C_{d,inner} &= 2\pi\varepsilon_0\varepsilon_r L_D/\ln(r_2/r_1), \\ C_{d,outer} &= 2\pi\varepsilon_0\varepsilon_r L_D/\ln(r_4/r_3), \text{ and} \\ C_d &= \frac{C_{d,inner}C_{d,outer}}{C_{d,inner}+C_{d,outer}} \end{aligned} \tag{2}$$

and the capacitance of the DBD lamp is given by

$$C_{DBD} = \frac{C_g C_d}{C_g + C_d} \tag{3}$$

where $\varepsilon_0 = 8.85 \times 10^{-12}\,\mathrm{F\,m^{-1}}$ represents the permittivity of free space, and ε_r is the relative permittivity of the quartz tube. By substituting the lamp parameters, the equivalent capacitance values are calculated; the results are listed in table 1.

2.2. Pulse generator

As the DBD lamp is mainly a capacitive load, the generation of pulses requires both high currents to charge the lamp capacitance and also techniques to release the energy stored in the lamp capacitance in order to terminate the pulse. What's more, the voltage amplitude of the pulses should reach several kilovolts to ignite the DBD lamp. The radiant power is almost proportional to the repetition rate. Therefore, a high repetition rate is needed to achieve high radiant power. A Marx generator with active recharging switches is suitable enough to excite the DBD lamp, as shown in figure 2 [24, 25].

In the charging mode, switches S_{DC}, S_{ci} are on and S_{di} are off. Capacitors C_i are charged by a constant current source in parallel. In the discharging period, switches S_{DC}, S_{ci} are off and S_{di} are on. Capacitors C_i are connected in series and a positive voltage is applied to the DBD lamp. In addition, the DBD lamp is short circuited by S_{ci} during the charging period. Thus, the energy stored in the lamp capacitance is released at the beginning of the charging mode. In this way, the voltage pulse is terminated and a steep falling edge is obtained.

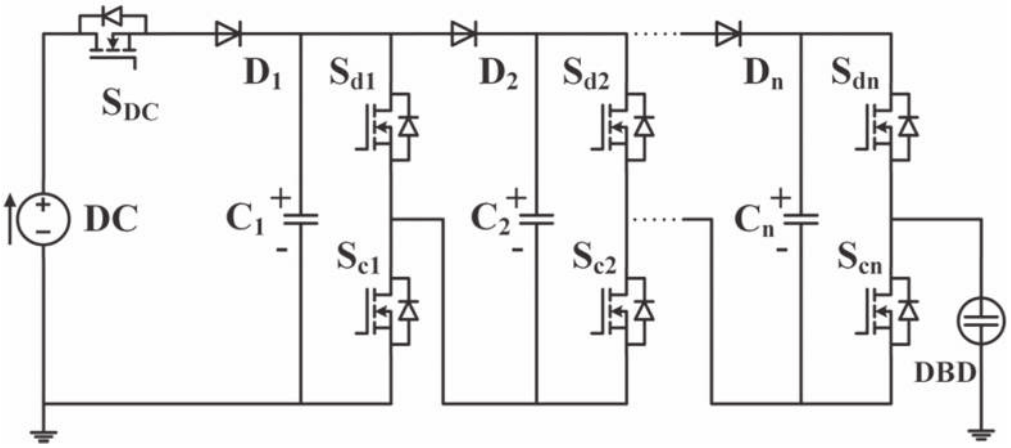

Figure 2. All-solid-state Marx generator with n stages to excite the $KrCl^*$ excimer DBD lamp.

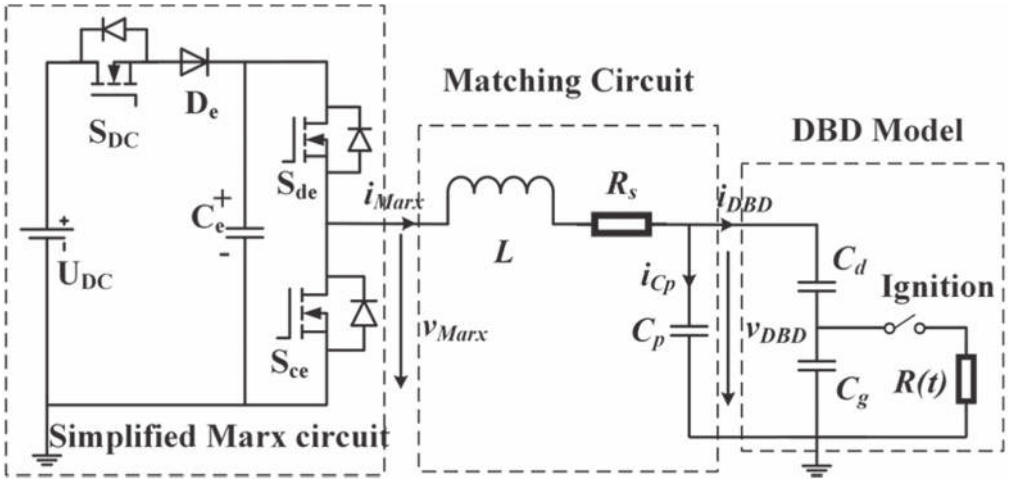

Figure 3. DBD lamp driven by the pulse generator with impedance matching circuit.

A Marx generator laboratory prototype was implemented. It operated within the voltage amplitude from 0–5.5 kV. The pulse width can be adjusted from 2 to 20 μs, and the repetition rate from 0.1 to 50 kHz. The pulse rise and fall times were both about 20 ns.

3. Impedance matching circuits analysis

The DBD lamp is mainly capacitive. If a capacitive load is directly connected to a voltage pulse generator, large charging and discharging currents will be produced. This causes serious electromagnetic interference (EMI), large turn on loss for MOSFETs, and has a risk of exceeding the maximum current of MOSFETs. Therefore, the primary goal of the matching circuit is to limit the output current of the Marx generator i_{Marx} illustrated in figure 3. i_{Marx} should be small at the rising edge of the Marx output voltage v_{Marx} to reduce switching loss.

What's more, a large DBD current i_{DBD} should be provided at ignition through the matching circuit to enhance the discharge of the DBD lamp.

Fast rising/falling edges and a large overshoot of the DBD voltage v_{DBD} are good for the discharge. This is the third goal for the matching circuit.

Inductive current limitation is superior to resistive current limitation in efficiency and rise time. Therefore, only inductive current limitation is considered. R_{s} in figure 3 is the stray resistance of the circuit. In addition, the capacitor in parallel to the DBD lamp could dramatically enhance the discharge energy support. We will analyze their performance in detail below. As the falling edge of the pulse is almost symmetrical to the rising edge, we will focus on the rising edge for simplicity.

3.1. RLC network

Figure 4(a) illustrates a simplified circuit with a current limiting inductor L. R is the resistance of the inductor winding. In order to obtain a fast voltage slope and high voltage overshoot at the capacitive load, the circuit is designed to achieve an underdamped system. Thus, the voltage across the capacitor and current through the capacitor are given by

$$v_{\mathrm{C}}(t) = V_{\mathrm{s}}\left[1 - \mathrm{e}^{-\alpha t}\left(\frac{\alpha}{\omega_{\mathrm{d}}}\sin(\omega_{\mathrm{d}}t) + \cos(\omega_{\mathrm{d}}t)\right)\right], \quad (4)$$

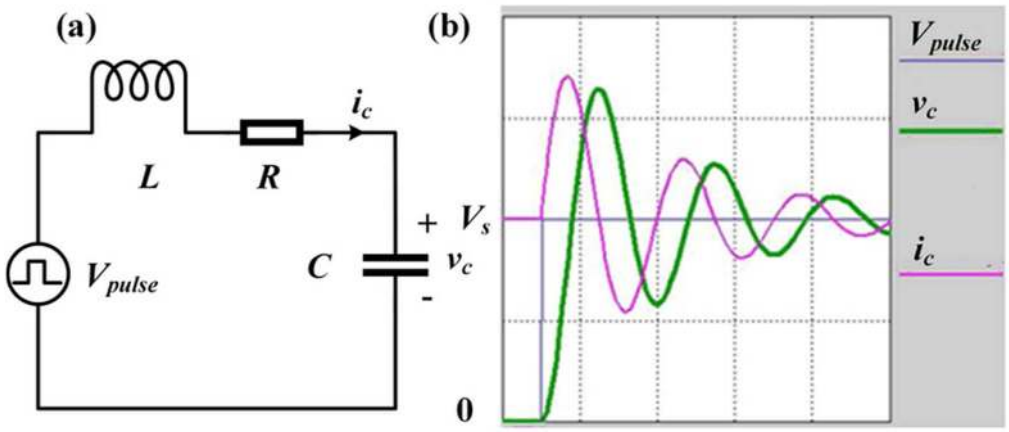

Figure 4. (a) Simplified circuit with a current limiting inductance. (b) Typical voltage and current waveforms.

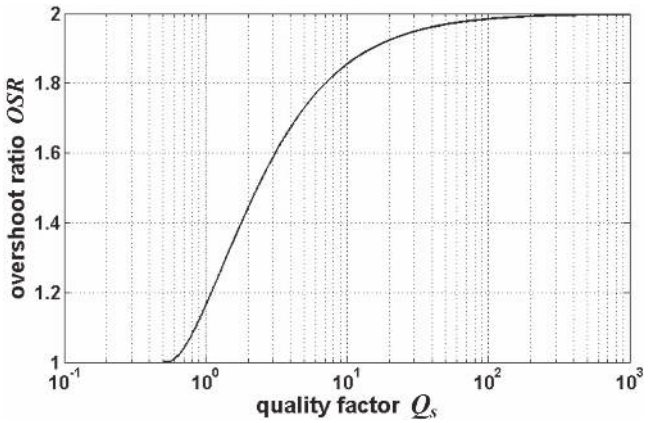

Figure 5. Overshoot ratio OSR dependent on the quality factor Q_s.

$$i_C(t) = \frac{V_s \sin(\omega_d t) e^{\alpha t}}{L\omega_d}, \tag{5}$$

where $\alpha = \dfrac{R}{2L}$, $\omega_0 = \dfrac{1}{\sqrt{LC}}$, $\omega_d = \sqrt{\omega_0^2 - \alpha^2}$.

The corresponding voltage and current waveforms are shown in figure 4(b).

3.1.1. Overshoot. In our previous work [23], we found that the radiant power of the DBD lamp increases with the applied voltage amplitude. Thus an interesting point is which overshoot factor could be achieved theoretically. From equation (4), the first peak of the capacitor voltage can be achieved at time $t = \pi/\omega_d$:

$$V_{C,pk} = V_s \left(1 + e^{-\alpha \frac{\pi}{\omega_d}}\right). \tag{6}$$

The circuit's quality factor is related to the circuit attenuation α as follows:

$$Q_s = \frac{1}{R}\sqrt{\frac{L}{C}} = \frac{L}{R}\sqrt{\frac{1}{LC}} = \frac{\omega_0}{2\alpha}, \tag{7}$$

By inserting equation (7) into (6), we obtain the dependence of the overshoot ratio from the circuit's quality factor:

$$\mathrm{OSR} = \frac{V_{C,pk}}{V_s} = 1 + e^{-\pi/\sqrt{4Q_s^2 - 1}}. \tag{8}$$

Equation (8) is illustrated by figure 5. The RLC circuit is underdamped when $Q_s > 0.5$. Thus, the OSR begins from $Q_s > 0.5$. In order to get a high voltage overshoot, Q_s should be large enough. The minimum quality factor is defined as $Q_s = 10$, which corresponds to a voltage gain of 1.85.

3.1.2. Rise time. For a high Q_s circuit, $\omega_d \approx \omega_0$, $T = 2\pi/\omega_0 = 2\pi\sqrt{LC}$. Therefore, the rise time t_r of voltage pulse is

$$t_r \propto 2\pi\sqrt{LC}, \tag{9}$$

C is the capacitance of DBD lamp and its value is relatively fixed. Thus, the rise time t_r increases with inductance L. However, according to previous research [23, 26], the radiant power and system efficiency increase with faster rise time.

3.1.3. Current limiting effect. The moment of the first current half wave's maximum is derived by setting the differential equation of (5) equal to zero. Then we have

$$t_{i=\max} = \frac{\arctan(\omega_d/\alpha)}{\omega_d} = \frac{\arctan(\sqrt{4Q_s^2 - 1})}{\omega_d} \tag{10}$$

and the corresponding maximum current is

$$i_{C,max} = \frac{V_s}{L\omega_d} \sin\left(\arctan\left(\frac{\omega_d}{\alpha}\right)\right) e^{-\frac{\alpha}{\omega_d}\arctan\left(\frac{\omega_d}{\alpha}\right)}. \tag{11}$$

For a high Q_s circuit, $\arctan(\sqrt{4Q_s^2 - 1}) \approx \dfrac{\pi}{2}$, $\omega_d \approx \omega_0$, thus

$$t_{i=\max} \approx \frac{\pi}{2\omega_0} = \frac{\pi}{2}\sqrt{LC},\ i_{C,max} = \frac{V_s}{L\omega_0} = \frac{V_s}{\sqrt{L/C}}.$$

The rise time of the Marx generator is about 20 ns, i.e. $t_{r,Marx} \approx 20$ ns. In order to reduce switching loss, $t_{i=max}$

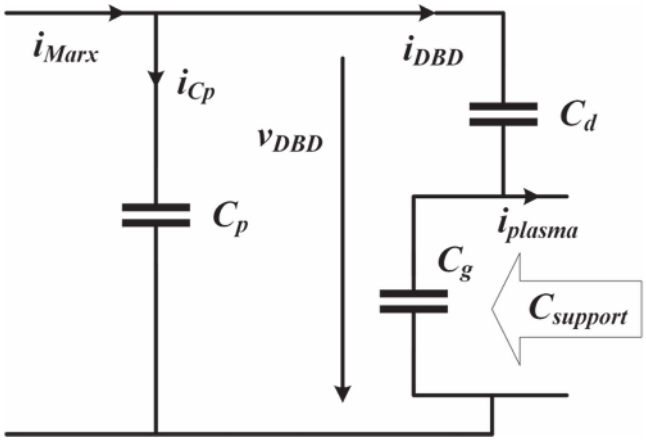

Figure 6. Discharge support by the parallel capacitance.

should be larger than $t_{r,Marx}$, i.e. $t_{i=max} \geqslant t_{r,Marx}$. The capacitance of the DBD lamp C can be derived through the geometrical structure or measured by an LCR meter. Therefore, one constraint condition that the inductor should meet is

$$L \geqslant \frac{4t_{r,Marx}^2}{\pi^2 C}. \tag{12}$$

What's more, $i_{C,max}$ should be smaller than the maximum current of MOSFETs I_D. Thus, another constraint condition for the inductor is

$$L \geqslant \frac{CV_s^2}{I_D^2}. \tag{13}$$

In summary, an increasing inductance results in larger voltage overshoot and better current limiting effect, which benefit radiant power and system efficiency. But the increase of inductance also leads to a larger rise time. Therefore, we need to find a tradeoff.

3.2. Parallel capacitor

The insertion of an inductor between the pulse generator and DBD lamp could limit the output current of the Marx generator, i_{Marx}. It is beneficial for the pulse generator in terms of switching loss and EMI. However, the DBD current i_{DBD} is also limited, and the achievable peak current and current slope have an influence on lamp efficiency and homogeneity. Adding a capacitance in parallel to the DBD lamp provides an extra voltage source to support the discharge energy.

As illustrated in figure 6, the discharge energy is provided by a current source i_{Marx} fed by the series inductor and a charge transfer from C_g to the plasma for a bare DBD. If the DBD lamp is equipped with an external parallel capacitor C_p, three sources provide energy to the plasma. Besides the current source i_{Marx}, C_g and C_p transfer charge to the plasma. The equivalent capacitance accessible by the discharge is enlarged to:

$$C_{support} = C_g + \frac{C_p C_d}{C_p + C_d}. \tag{14}$$

The equivalent series capacitance of C_p and C_d, i.e. C_{eq}, should be larger than C_g to effectively support the discharge. In addition, C_{eq} increases with C_p, as shown in figure 7. It seems that If C_p is larger, then there will be more energy to support the plasma. However, larger C_p also enhances the total capacitance that has to be driven by the pulse generator. What's more, the growth rate of C_{eq} slows down with larger C_p. Thus, C_{eq} should be smaller than $C_d/2$. The valid range of C_{eq} is marked by the red line shown in figure 7.

For a bare DBD, the plasma current in the discharge gap is

$$\begin{aligned} i_{plasma} &= \left(1 + \frac{C_g}{C_d}\right) i_{Marx}(t) - C_g \frac{dv_{DBD}(t)}{dt} \\ &= \frac{C_g}{C_{DBD}} i_{Marx}(t) - C_g \frac{dv_{DBD}(t)}{dt}. \end{aligned} \tag{15}$$

For a DBD with attached parallel capacitor, the plasma current in the discharge gap is

$$i_{plasma,C_p} = \frac{C_g}{C_{DBD}} i_{Marx}(t) - \frac{C_{DBD} + C_p}{C_{DBD}} C_g \frac{dv_{DBD}(t)}{dt}. \tag{16}$$

When the external current $i_{Marx}(t)$ remains constant, the internal voltage source support is enhanced by a factor of $(C_{DBD} + C_p)/C_{DBD}$.

When the impedance matching circuit composed of a series inductor and parallel capacitor is employed, the theoretical analysis in section 3.1 still works, but the capacitor $C = C_{DBD} + C_p$.

4. Experimental set-up

Figure 8 shows the experimental setup. The KrCl* excimer DBD lamp was driven by a pulse generator through three different impedance matching circuits: series inductor, parallel capacitor, and series inductor combined with parallel capacitor, respectively. A high voltage probe (Tektronix P6015A, 1000:1, rise time 5 ns) and a current probe (Pearson P4100, 1 V A^{-1}, rise time 10 ns) were connected to a digital oscilloscope (Agilent Technologies MSO-X 3024A, bandwidth 200 MHz, sample rate 4 GSa s^{-1}) to measure the voltage and current waveforms of the DBD lamp [27].

The input power P_{in} of the pulse generator from the power grid was measured by a power meter (PF9901).

A sensor (Hamamatsu, H8025-222) of the UV power meter (Hamamatsu c8026) was used to detect the 222 nm irradiance of the KrCl* excilamp. The radiant power P_{rad} of 222 nm is calculated according to Keiz formula [28]:

$$P_{rad} = \frac{2\pi^2 D L_D}{2\alpha + \sin(2\alpha)} E, \tag{17}$$

where E is the measured irradiance (W m^{-2}). The irradiance was recorded on average, over 60 s continuously, with a sample interval of 1 s. D represents the distance (m) from the lamp axis to the UV sensor; L_D refers to the effective discharge length (m) of the lamp; and α is the half angle (radians) subtended by the DBD lamp at the sensor position, i.e. $\tan\alpha = L_D/(2D)$. In our experiments, L_D was 0.14 m, and D was set as 0.5 m.

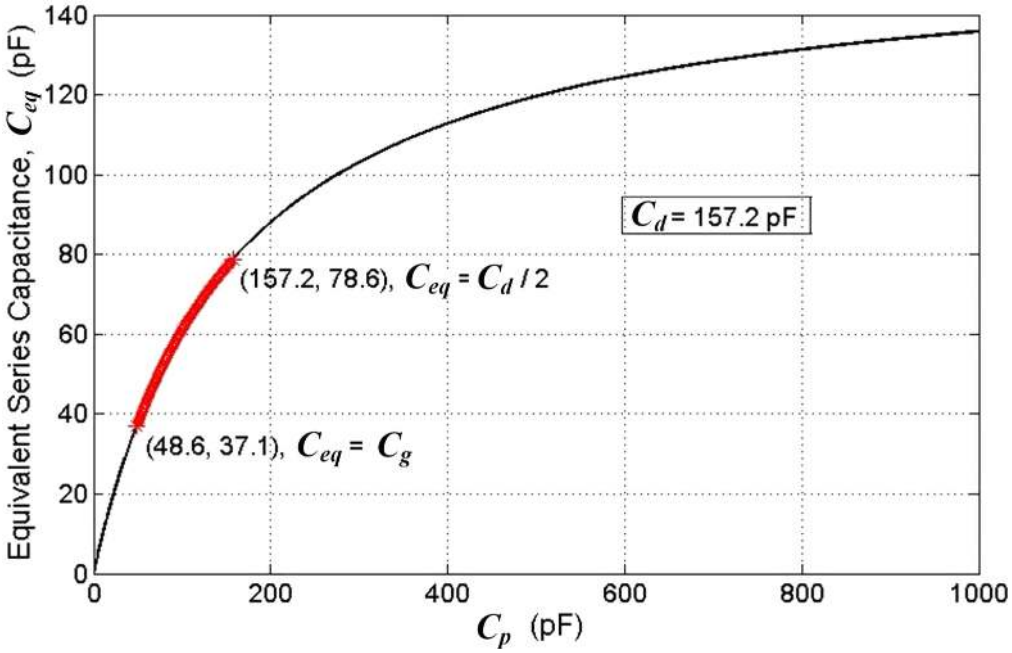

Figure 7. Equivalent series capacitance of C_p and C_d dependent on C_p. ($C_d = 157$ pF.)

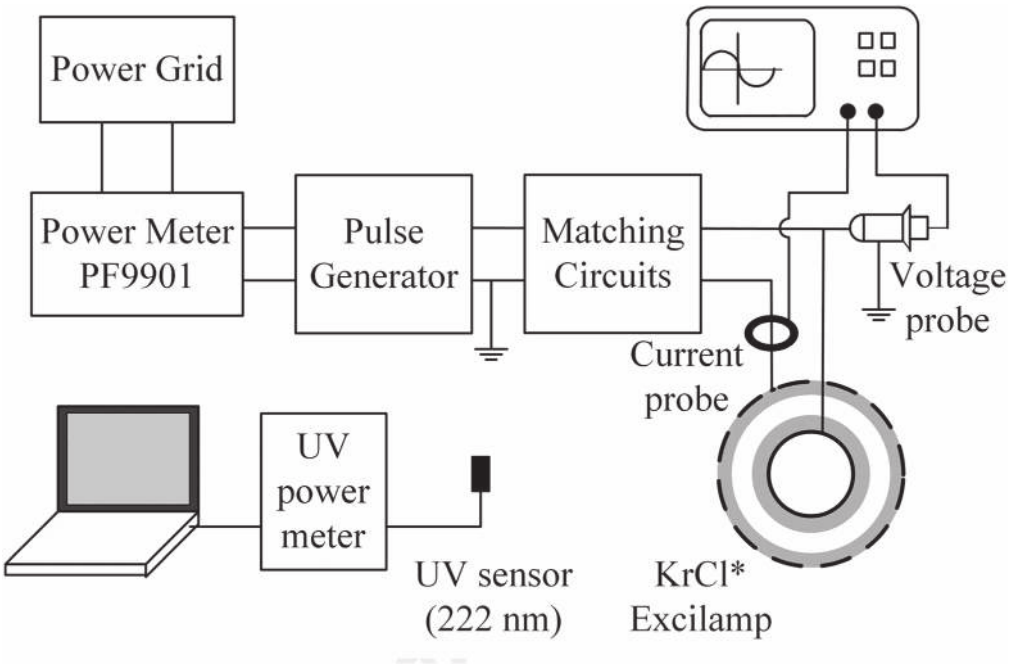

Figure 8. Schematic diagram of the experimental setup.

The system efficiency can be derived from the ratio of measured radiant power P_{rad} and input power of the pulse generator P_{in}:

$$\eta = P_{rad}/P_{in}. \quad (18)$$

When voltage pulses with the same amplitude, pulse width, and repetition rate are fed into different impedance matching circuits, the radiant power of the DBD lamp and system efficiency could be used to evaluate the performance of the matching circuits.

5. Experimental results and discussion

First, we used the homemade pulse generator to drive the DBD lamp directly. The pulse generator operated at a voltage amplitude of 1150 V, with a pulse width of 2 μs and a

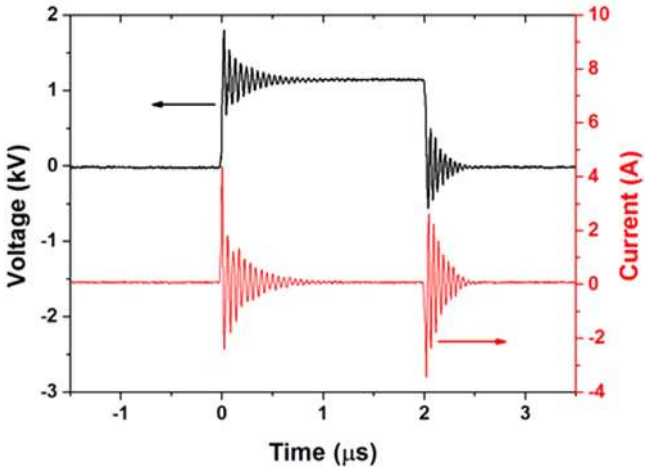

Figure 9. Voltage and current waveforms of the DBD lamp excited by a pulse generator. The voltage amplitude is not high enough to ignite the lamp.

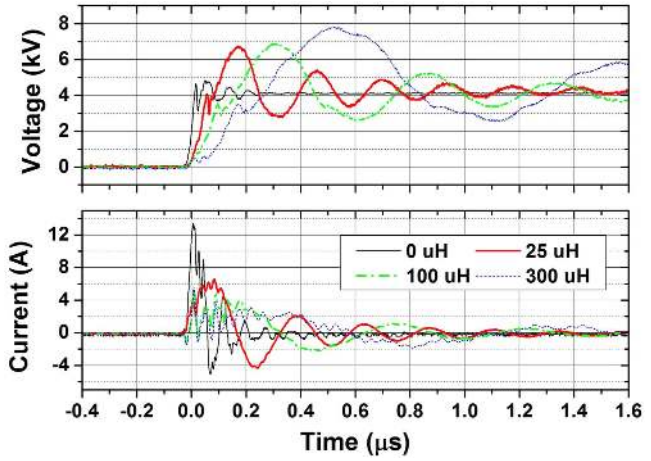

Figure 10. Typical voltage and current waveforms with different series inductors.

repetition rate of 50 kHz. It is found that a serious oscillation at a frequency of 17.73 MHz occurs before the ignition of the lamp, as shown in figure 9. The oscillation is caused by stray inductance, stray resistance and lamp capacitance. The lamp capacitance was measured to be 32.57 pF by an LCR meter, which is consistent with the calculated result in table 1. According to equation (5) and the measured current waveforms, the values of stray inductance and resistance were calculated to be 2.68 μH and 21.19 Ω, respectively.

5.1. Series inductor

The minimum series inductance could be determined by equations (7), (12), and (13). R in equation (7) was set as 21.19 Ω. $t_{r,Marx}$ was set as 20 ns based on experimental results. According to the datasheet of MOSFET, I_D was 24 A. C equalled the DBD capacitance, i.e. 32 pF. The minimum inductance was calculated to be 20 μH.

In order to test the performance of the inductor, several inductors with different values were employed; the minimum inductance was 5 μH, the maximum was 350 μH. The pulse

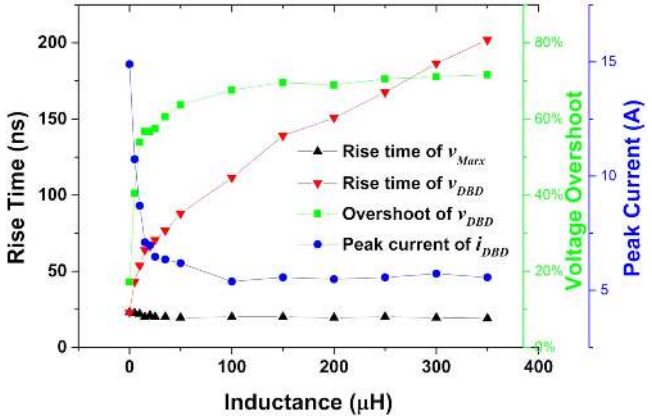

Figure 11. Series inductance dependence of the electrical parameters.

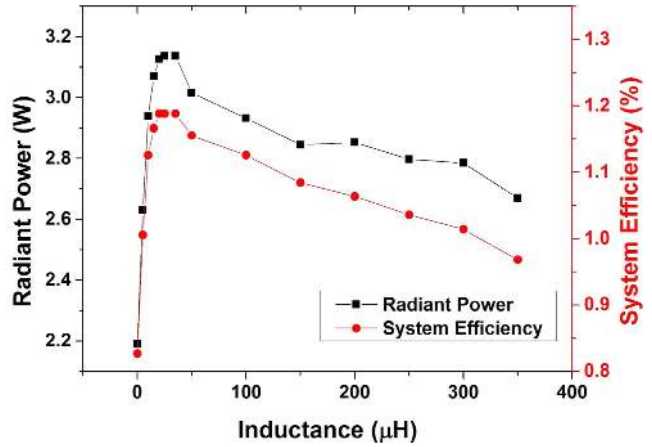

Figure 12. Series inductance dependence of radiant power and system efficiency.

generator operated at a voltage amplitude of 4.10 kV, with a pulse width of 2 μs and a repetition rate of 50 kHz. In the following experiments, the operation conditions of the pulse generator were fixed.

Typical voltage and current waveforms of the DBD lamp are shown in figure 10. Compared with driving the DBD lamp directly, the insertion of inductors could obviously slow down the voltage rise time and enlarge the voltage overshoot. In addition, the amplitude of the DBD current decreases a lot, especially during the rising edge of the Marx output voltage, which reduces switching loss.

The electrical parameters dependent on series inductance are shown in figure 11. The rise time of the Marx output voltage v_{Marx} is almost independent of inductance. In fact, with the insertion of inductors, the rise time of v_{Marx} decreases from 23 to 20 ns. However, the rise time of the DBD voltage v_{DBD} increases with inductance. When the inserted inductance is smaller than 50 μH, the overshoot of v_{DBD} increases from 17.20% to 63.70% quickly with inductance. After that, the overshoot increases slowly. The peak value of the DBD current i_{DBD} decreases from 14.9 to 6.19 A quickly when the inserted inductance is smaller than 50 μH. Then the peak current of i_{DBD} decreases slowly with increasing inductance.

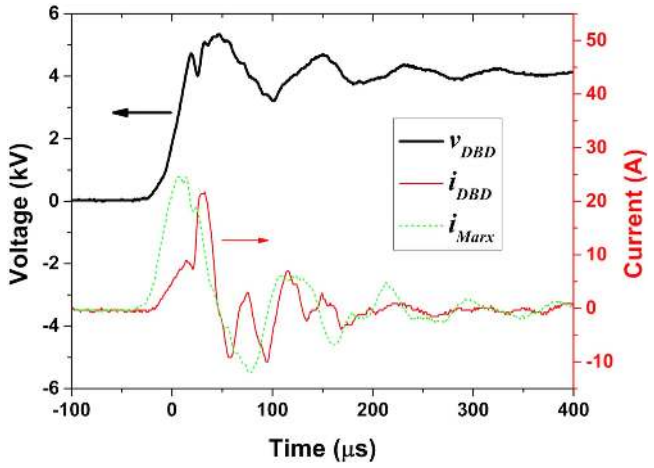

Figure 13. Typical voltage current waveforms with a 100 pF parallel capacitor.

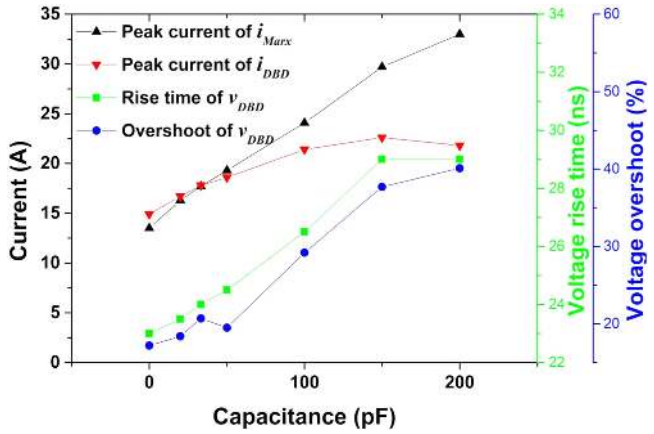

Figure 14. Parallel capacitance dependence of the electrical parameters.

Figure 12 shows that radiant power and system efficiency increase quickly with inductance first, and then decrease slowly. The peak radiant power and system efficiency are 3.14 W and 1.19% respectively, reaching at 25 μH series inductance. Compared with driving the DBD lamp with a pulse generator directly, an increase of 43.2% in radiant power and an increase of 43.7% in system efficiency are achieved. According to figure 12, a minimum inductance that meets equations (7), (12), and (13) is enough. A larger inductance degrades the performance of the DBD discharge.

5.2. Parallel capacitor

As analyzed in section 3.2, capacitors paralleled with the DBD lamp could increase the discharge current. In this section, capacitors with different values were paralleled with the DBD lamp directly.

Typical voltage and current waveforms of the DBD lamp with a 100 pF parallel capacitor are shown in figure 13. It demonstrates that the parallel capacitor enlarges the discharge current. However, the Marx current enlarges at the same time, which increases switching loss.

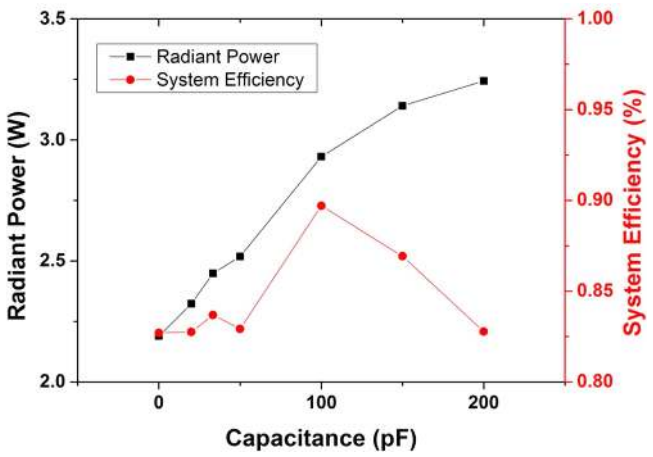

Figure 15. Parallel capacitance dependence of radiant power and system efficiency.

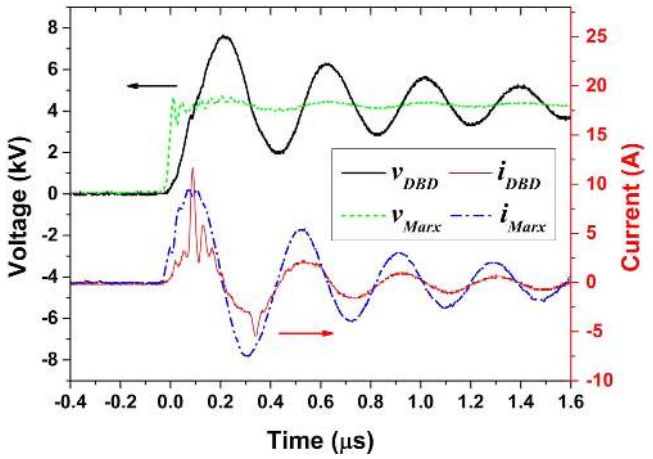

Figure 16. Typical voltage and current waveforms with a 25 μH series inductor and a 100 pF parallel capacitor.

Figure 14 illustrates the electrical parameters dependent on parallel capacitance. With the increase of parallel capacitance, the peak current of the Marx generator increases continually. However, the peak current of i_{DBD} increases first, and then no longer increases. One possible reason is that the stray inductance and resistance between external capacitor and DBD lamp limited the DBD current. The rise time and overshoot of v_{DBD} increase with the parallel capacitance too.

The radiant power increases with parallel capacitance continually, as illustrated in figure 15. However, the growth rate decreases dramatically when the parallel capacitor is larger than 100 pF. The system efficiency increases with parallel capacitance first, and then decreases. The peak system efficiency is 8.48% higher than bare DBD, arriving at 100 pF parallel capacitor.

5.3. Inductor combined with capacitor

According to the above analysis and experimental results, both a series inductor and parallel capacitor could improve the radiant power and system efficiency. However, a series inductor limits the discharge current and a parallel capacitor

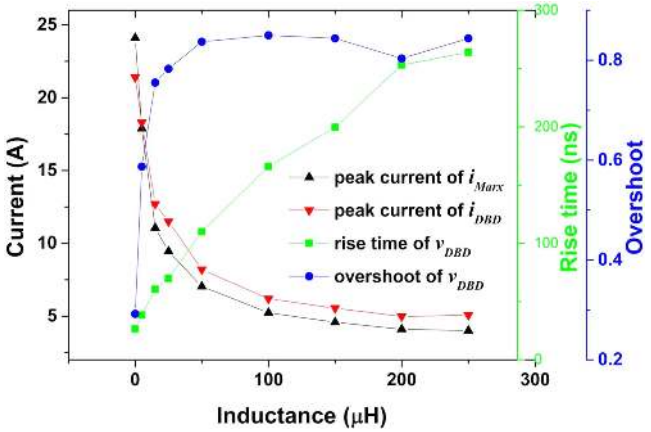

Figure 17. Electrical parameters dependent on the series inductance.

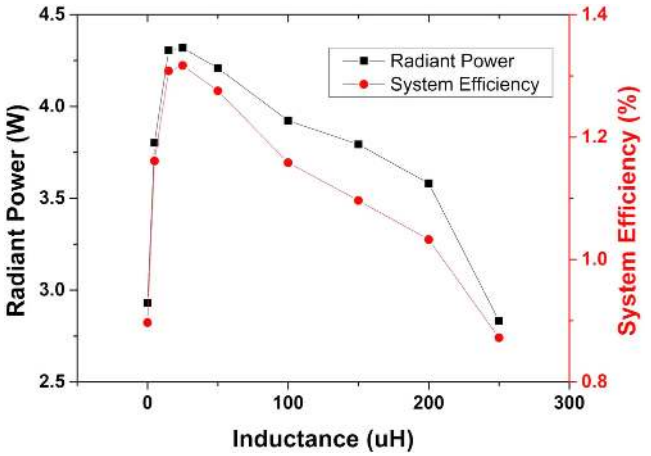

Figure 18. Radiant power and system efficiency dependent on the series inductance.

enlarges the Marx current. A series inductor combined with a parallel capacitor is a good solution. The Marx current could be limited by a series inductor while the DBD current could be enlarged by a parallel capacitor.

Since the highest system efficiency is achieved with a 100 pF parallel capacitor in figure 15, the parallel capacitance was fixed to be 100 pF. Several inductors with different values were employed to find the best point where the highest radiant power and system efficiency could be achieved.

Typical voltage and current waveforms are shown in figure 16. A 25 μH series inductor combined with a 100 pF parallel capacitor was inserted between the pulse generator and DBD lamp. The DBD current i_{DBD} is enlarged significantly at ignition. It is obvious that multiple discharges occur. What is more, the Marx current i_{Marx} is relatively small during the rising edge of the Marx voltage v_{Marx}. These features are beneficial to both the pulse generator and DBD discharge.

As shown in figure 17, when the series inductance is smaller than 50 μH, the peak currents of i_{Marx} and i_{DBD} decrease rapidly with increasing inductance. After that, i_{Marx} and i_{DBD} decrease slowly. An interesting phenomenon is that the peak value of i_{DBD} is always larger than that of i_{Marx} with the help of a series inductor combined with a parallel capacitor. The overshoot of the DBD voltage v_{DBD} increases quickly with inductance when the series inductance is smaller than 50 μH. After that, it is almost unchanged. However, rise time of v_{DBD} keeps increasing with inductance. Therefore, a series inductance that is smaller than 50 μH is preferred.

Figure 18 shows that radiant power and system efficiency increase first with inductance and then decrease. The peak radiant power and system efficiency are 4.32 W and 1.32% respectively, reaching 25 μH series inductance. Compared with exciting the DBD lamp with a pulse generator directly, an increase of 97.3% in radiant power and an increase of 59.3% in system efficiency are achieved.

Compared with using a series inductor or parallel capacitor alone, a series inductor combined with a parallel capacitor makes the best performance.

6. Conclusion

In this paper, different matching networks (series inductor, parallel capacitor, and series inductor combined with parallel capacitor) are analyzed. The results show that a series inductor could limit the current at the rising edge of the Marx output voltage. Thus, switching loss is reduced. However, a discharge current at ignition is also limited. The voltage overshoot is enlarged whereas the rise time increased. A parallel capacitor could provide a large discharge current at ignition. However, the output current of the pulse generator is also enlarged at the same time, which increases the switching loss. A series inductor combined with a parallel capacitor turns out to be a good solution, with its full advantages of inductor and capacitor. In addition, the methods to calculate the value of the series inductor and parallel capacitor are given.

Experiments with these three different matching networks were conducted, and the experimental results match the theoretical analysis well. It also demonstrates that the radiant power and system efficiency increase with inductance first, and then decrease. The radiant power increases with parallel capacitance. However, the system efficiency increases first, and then decreases. A series inductor combined with a parallel capacitor gives the best performance not only in radiant power and system efficiency, but also in the switching loss of the pulse generator. Compared with the DBD lamp directly excited by a pulse generator, an increase of 97.3% in radiant power and an increase of 59.3% in system efficiency are achieved through this matching circuit.

Although the theoretical analysis and experiments were conducted with a DBD lamp, the conclusions could also be suitable for other DBD reactors excited by pulse generators.

Acknowledgments

This work was supported by National Natural Science Foundation of China under the Grant No. 51277033.

References

[1] Borcia G, Anderson C A and Brown N M D 2003 *Plasma Source Sci. Technol.* **12** 335
[2] Mericam-Bourdet N *et al* 2012 *Eur. Phys. J. Appl. Phys.* **57** 30801
[3] Wei L S *et al* 2016 *Plasma Sci. Technol.* **18** 147
[4] Bhattacharyya A and Rajanikanth B S 2015 *IEEE Trans. Dielectr. Electr. Insul.* **22** 1879
[5] Wu H X, Fang Z and Xu Y H 2015 *Plasma Sci. Technol.* **17** 228
[6] Li Y *et al* 2016 *Plasma Sci. Technol.* **18** 173
[7] Han Q Y *et al* 2013 *J. Phys. D: Appl. Phys.* **46** 505203
[8] Lomaev M I, Sosnin E A and Tarasenko V F 2012 *Prog. Quant. Electron.* **36** 51
[9] Sosnin E A, Oppenländer T and Tarasenko V F 2006 *J. Photochem. Photobiol.* C **7** 145
[10] Meiße M 2013 Resonant behaviour of pulse generators for the efficient drive of optical radiation sources based on dielectric barrier discharges *PhD thesis* KIT Karlsruhe, Germany
[11] Liu S H and Neiger M 2001 *J. Phys. D: Appl. Phys.* **34** 1632
[12] Williamson J M *et al* 2006 *J. Phys. D: Appl. Phys.* **39** 4400
[13] Merbahi N *et al* 2007 *J. Appl. Phys.* **101** 123309
[14] Xiong Q *et al* 2010 *Phys. Plasmas* **17** 043506
[15] Cheng H *et al* 2016 *High Volt.* **1** 62
[16] Shao T *et al* 2008 *J. Phys. D: Appl. Phys.* **41** 215203
[17] Jiang H *et al* 2011 *IEEE Trans. Plasma Sci.* **39** 2076
[18] Chen Z Y 2002 *IEEE Trans. Plasma Sci.* **30** 1922
[19] Singh K P and Roy S 2007 *Appl. Phys. Lett.* **91** 081504
[20] Shin Y C, Kim B and Ko K C 2010 Considerations on the DBD power supply for surface change of ozone reactor *2010 IEEE Int. Power Modulator and High Voltage Conf. (Atlanta, GA)* (Piscataway, NJ: IEEE) pp 679–85
[21] Opaits D F *et al* 2008 *J. Appl. Phys.* **104** 043304
[22] Rao J F, Liu K F and Qiu J 2013 *IEEE Trans. Plasma Sci.* **41** 564
[23] Wang Y G *et al* 2016 *IEEE Trans. Plasma Sci.* **44** 1933
[24] Wang Y G *et al* 2014 Repetitive high voltage all-solid-state Marx generator for dielectric barrier discharge pulsed plasma *2014 IEEE Int. Power Modulator and High Voltage Conf. (Santa Fe, NM)* (Piscataway, NJ: IEEE) pp 648–51
[25] Zhou Z W *et al* 2016 *IEEE Trans. Plasma Sci.* **44** 2779
[26] Tastekin D *et al* 2011 Pulsed voltage converter with bipolar output voltages up to 10 kV for dielectric barrier discharge *2011 IEEE 8th Int. Conf. on Power Electronics and ECCE (Asia Jeju, Korea)* (Piscataway, NJ: IEEE) pp 1558–65
[27] Tarasenko V F and Rybka D V 2016 *High Volt.* **1** 43
[28] Zhuang X B *et al* 2010 *J. Phys. D: Appl. Phys.* **43** 205202